Inorg. Chem. **2004**, *43*, 3854–3862

Ligand Displacement and Oxidation Reactions of Methyl(oxo)rhenium(V) Complexes

Xiaopeng Shan, Arkady Ellern, Ilia A. Guzei,† and James H. Espenson*

Ames Laboratory and Department of Chemistry, Iowa State University, Ames, Iowa 50011

Received February 19, 2004

Compounds that contain the anion $[MeReO(edt)(SPh)]^-$ (**3**$^-$) were synthesized with the countercations 2-picolinium (PicH$^+$**3**$^-$) and 2,6-lutidinium (LutH$^+$**3**$^-$), where edt is 1,2-ethanedithiolate. Both PicH$^+$**3**$^-$ and MeReO(edt)(tetramethylthiourea) (**4**) were crystallographically characterized. The rhenium atom in each of these compounds exists in a five-coordinate distorted square pyramid. In the solid state, PicH$^+$**3**$^-$ contains an anion with a short (d_{SH} = 232 pm) and nearly linear hydrogen-bonded (N–H···S) interaction to the cation. Ligand substitution reactions were studied in chloroform. Displacement of PhSH by PPh_3 follows second-order kinetics, $d[MeReO(edt)(PPh_3)]/dt = k[PicH^+\mathbf{3}^-][PPh_3]$, whereas with pyridines an unusual form was found, $d[MeReO(edt)(Py)]/dt = k[PyH^+\mathbf{3}^-][Py]^2$, in which the conversion of PicH$^+$**3**$^-$ to PyH$^+$**3**$^-$ has been incorporated. Further, added Py accelerates the formation of $[MeReO(edt)(PPh_3)]$, $v = k\cdot[PicH^+\mathbf{3}^-]\cdot[PPh_3]\cdot[Py]$. Compound **4**, on the other hand, reacts with both PPh_3 and pyridines, L, at a rate given by $d[MeReO(edt)(L)]/dt = k\cdot[\mathbf{4}]\cdot[L]$. When PicH$^+$**3**$^-$ reacts with pyridine *N*-oxides, a three-stage reaction was observed, consistent with ligand replacement of SPh$^-$ by PyO, N–O bond cleavage of the PyO assisted by another PyO, and eventual decomposition of MeRe(O)(edt)(OPy) to $MeReO_3$. Each of first two steps showed a large substituent effect; Hammett analysis gave $\rho_1 = -5.3$ and $\rho_2 = -4.3$.

Introduction

Oxorhenium(V) compounds are effective catalysts for oxygen atom transfer, OAT.[1−8] In the general case the reaction can be written as YO + X → Y + XO; in the reactions under consideration here, pyridine *N*-oxides and triphenylphosphine were used

$$PyO + PPh_3 \rightarrow Py + Ph_3PO \qquad (1)$$

for which $\Delta G^\circ = -256$ kJ when, for example, PyO = 4-MeC_5H_4NO. (The identity of the PyO is not highly pertinent because BDE(4-XC_5H_4N-O) is nearly substituent-independent.)[9] Despite its thermodynamic spontaneity, the reaction presents so large a kinetic barrier as to be entirely negligible in rate. The rhenium-catalyzed reaction is useful in practice for the deoxygenation of N-heterocycles: gram-scale conversions have been realized for a wide range of PyO reagents in reactions run in ambient conditions.[5] Of greater interest is the mechanism by which the catalysts function. The stoichiometric reactions and certain mechanistic aspects for the rhenium reagents are analogous to those catalyzed by molybdenum oxotranferases.[10]

One fact already made clear is that ligand substitution (LS) precedes OAT, it being the step that introduces the O-atom donor into the coordination shell of rhenium in place of the ligand originally present. It has proved informative to study LS separately from OAT. Phosphines, pyridines, and *N*-heterocycles in general have been useful ligands in the context of LS reactions, in that subsequent reactions do not take place.[1,11−14]

* Corresponding author. E-mail: Espenson@iastate.edu.
† Department of Chemistry, University of Wisconsin, Madison, Wisconsin 53706.

(1) Espenson, J. H.; Nabavizadeh, S. M. *Eur. J. Inorg. Chem.* **2003**, 1911−1916.
(2) Dixon, J.; Espenson, J. H. *Inorg. Chem.* **2002**, *41*, 4727−4731.
(3) (a) Lente, G.; Espenson, J. H. *Inorg. Chem.* **2000**, *39*, 4809−4814. (b) Espenson, J. H. *Chem. Commun.* **1999**, 479−488. (c) Shan, X.; Ellern, A.; Guzei, I. A.; Espenson, J. H. *Inorg. Chem.* **2003**, *42*, 2362−2367.
(4) Shan, X.; Ellern, A.; Espenson, J. H. *Inorg. Chem.* **2002**, *41*, 7136−7142. (b) Arias, J.; Newlands, C. R.; Abu-Omar, M. M. *Inorg. Chem.* **2001**, *40*, 2185−2192.
(5) Wang, Y.; Espenson, J. H. *Org. Lett.* **2000**, *2*, 3525−3526.
(6) Wang, Y.; Espenson, J. H. *Inorg. Chem.* **2002**, *41*, 2266−2274.
(7) Koshino, N.; Espenson, J. H. *Inorg. Chem.* **2003**, *42*, 5735−5742. (b) Wang, Y.; Lente, G.; Espenson, J. H. *Inorg. Chem.* **2002**, *41*, 1272−1280.
(8) Abu-Omar, M. M.; Khan, S. I. *Inorg. Chem.* **1998**, *37*, 4979−4985.
(9) Luo, Y.-R. *Handbook of Bond Dissociation Energies in Organic Compounds*; CRC Press: Boca Raton, FL, 2003.
(10) (a) Holm, R. H. *Coord. Chem. Rev.* **1990**, *100*, 183−221. (b) Holm, R. H.; Berg, J. M. *Acc. Chem. Res.* **1986**, *19*, 363−370. (c) Coucouvanis, D. *Acc. Chem. Res.* **1991**, *24*, 1−8. (d) Sung, K.-M.; Holm, R. H. *J. Am. Chem. Soc.* **2001**, *123*, 1931−1943.

10.1021/ic049772c CCC: $27.50
Published on Web 06/04/2004

Chart 1

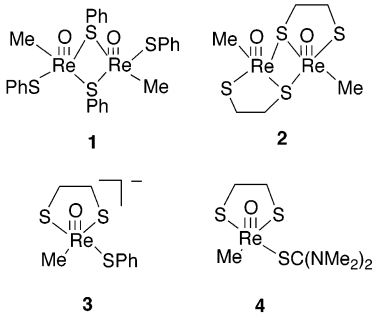

We have now extended this research by the synthesis of three new methyl(oxo)rhenium(V) complexes. Two contain the anion MeReO(edt)(SPh)$^-$ (**3**$^-$) with the cations 2-picolinium (PicH$^+$**3**$^-$) and 2,6-lutidinium (LutH$^+$**3**$^-$), and the third is the molecular rhenium compound, MeReO(edt)(SC(NMe$_2$)$_2$) (**4**), where edt stands for 1,2-ethanedithiolate.[15] Their structural formulas are shown in Chart 1.

Studies of the LS reactions with pyridines and PPh_3 have been undertaken. Unexpectedly, pyridines accelerate the LS reaction of PicH$^+$**3**$^-$ with PPh_3. Additionally, we have characterized the steps of OAT from pyridine *N*-oxides to triphenylphosphine, eq 1, including a study of the intermediates MeReO(edt)(OPy) from LS and MeRe(O)$_2$(edt)(OPy) from oxidation. The OAT portion of the study focuses especially on the finding that nucleophiles assist in the oxidation by incorporating a second molecule of pyridine *N*-oxide in the transition state.

Experimental Section

Reagents and Instrumentation. {MeReO(edt)}$_2$ (**2**) was synthesized from 1,2-ethanedithiol and {MeReO(benzenethiolate)$_2$}$_2$ (**1**),[16] the latter prepared according to the literature.[17] Other chemical reagents were purchased and used as received. Acetonitrile-d_3, benzene-d_6, and chloroform-d_1 were employed as solvents for NMR spectroscopy. Chloroform was used as the solvent for UV−vis and IR spectra and for kinetics.

UV−vis spectra and kinetic data were obtained with Shimadzu model 3101 and OLIS RSM stopped-flow spectrophotometers. A circulating water thermostatic system that controlled the temperature variation to within ±0.2 °C was used for the stopped-flow instrument, and an electronic thermostatic holder that maintained the temperature of the cell to ±0.2 °C was used for the UV−vis spectrophotometer. IR spectra were collected with a Nicolet-500 spectrometer. A Bruker DRX-400 MHz spectrophotometer was used to record ^{1}H and ^{13}C NMR spectra. The chemical shift for ^{1}H was calculated relative to the residual proton of the solvent, δ 1.94 for acetonenitrile-d_3, 7.16 for benzene-d_6, and 7.27 for chloroform-d_1. Elemental analyses were performed by Desert Analytics Laboratory.

Preparation of Salts of MeReO(edt)(SPh)$^-$ (3). 1,2-Ethanedithiol (18.8 mg, 16.8 μL, 0.2 mmol) was added to a mixture of **1** (87 mg, 0.1 mmol) and a pyridine (0.2 mmol of 2-picoline or 2,6-lutidine) in 20 mL of toluene, as in eq 2. The resulting solutions were stirred for 2 h as a dark red solid deposited. The product was collected by filtration, rinsed by hexanes, and dried under vacuum.

$$\frac{1}{2}\{MeRe(O)(SPh)_2\}_2 + Py + (C_2H_4)(SH)_2 \rightarrow [PyH][MeRe(O)(S_2C_2H_4)(SPh)] + PhSH \quad (2)$$

PicH$^+$**3**$^-$ was obtained in 97% yield. A crystal suitable for X-ray diffraction analysis was obtained by recrystallization from methylene chloride−hexanes. NMR (acetonitrile-d_3) ^{1}H: δ 8.48 (d, 1H), 8.41 (m, 1H), 7.81 (m, 2H), 7.57 (m, 2H), 7.23 (t, 2H), 7.10 (t, 1H), 2.88 (m, 1H), 2.73 (s, 3H), 2.67 (m, 2H), 2.49 (m, 1H), 2.18 (s, 3H). ^{13}C: 150.0, 147.0, 133.9, 128.3, 127.5, 124.8, 124.7, 43.6, 43.4, 19.3, 7.2. IR ($CHCl_3$), ν/cm^{-1}: Re−O, 1003; N−H and S−H, absent, until 2-MeC_5H_4Py had been added, when a broad, strong ν_{NH} was detected at 3125 cm^{-1}. UV−vis ($CHCl_3$), λ_{max}/nm (log ϵ): 337 (sh), 397 (3.48). Elemental analysis $C_{15}H_{20}NOReS_3$, found (calcd): C, 35.30 (35.14); H, 4.05 (3.93); N, 2.71 (2.73); S, 19.08 (18.76).

LutH$^+$**3**$^-$ was obtained in 90% yield. NMR (acetonitrile-d_3) ^{1}H: δ 8.26 (t, 1H), 7.57 (m, 4H), 7.23 (m, 2H), 7.11 (m, 1H), 2.88 (m, 1H), 2.69 (m, 2H), 2.67 (s, 6H), 2.17 (s, 3H). ^{13}C: 146.5, 133.9, 127.4, 125.0, 124.7, 43.6, 43.4, 18.8, 6.5. UV−vis ($CHCl_3$), λ_{max}/nm (log ϵ): 337 (sh), 369 (3.48).

Preparation of MeReO(edt)(tmtu) (4). Tetramethylthiourea (24.6 mg, 0.2 mmol) was mixed with **2** (61.9 mg, 0.1 mmol) in 20 mL of toluene. As the solution was stirred for 4 h, its color changed from brown to violet. Then, 20 mL of hexanes was layered on the top. After 1 day, black crystals appeared; they were filtered and rinsed by hexanes, giving a final yield of 76%. Crystals suitable for X-ray diffraction analysis were obtained. NMR (benzene-d_6) ^{1}H: δ 3.58 (m, 1H), 3.25 (s, 3H), 3.13 (m, 1H), 3.04 (m, 1H), 2.69 (m, 1H), 2.38 (sb, 12H). ^{13}C: 46.2, 43.2, 6.8. IR ($CHCl_3$), ν/cm^{-1}: Re−O, 976. UV−vis ($CHCl_3$), λ_{max}/nm: 300 (sh). Elemental analysis $C_7H_{19}N_2OReS_3$, found (calcd): C, 21.71 (21.76); H, 4.12 (4.34); N, 6.34 (6.34); S, 21.80 (21.78).

X-ray Crystallography. Crystals of PicH$^+$**3**$^-$ and **4**, selected under ambient conditions, were mounted and centered in the X-ray beam by using a video camera. The crystal evaluation and data collection were performed on a Bruker CCD-1000 diffractometer with Mo Kα (λ = 0.71073 Å) radiation and a detector-to-crystal distance of 4.90 cm. The cell constants were calculated from a set of a certain amount of strong reflections from the actual data collection. The data were collected by using the full sphere routine. This data set was corrected for Lorentz and polarization effects. The absorption correction was based on fitting a function to the empirical transmission surface as sampled by multiple equivalent measurements[18] using SADABS software.[19]

The position of the Re atom was found by the Patterson method. The remaining atoms were located in an alternating series of least-squares cycles and difference Fourier maps. All non-hydrogen atoms

(11) Lahti, D. W.; Espenson, J. H. *J. Am. Chem. Soc.* **2001**, *123*, 6014−6024.
(12) (a) Jacob, J.; Lente, G.; Guzei, I. A.; Espenson, J. H. *Inorg. Chem.* **1999**, *38*, 3762−3763. (b) Jacob, J.; Guzei, I. A.; Espenson, J. H. *Inorg. Chem.* **1999**, *38*, 1040−1041.
(13) Lente, G.; Guzei, I. A.; Espenson, J. H. *Inorg. Chem.* **2000**, *39*, 1311−1319.
(14) Espenson, J. H.; Shan, X.; Lahti, D. W.; Rockey, T. M.; Saha, B.; Ellern, A. *Inorg. Chem.* **2001**, *40*, 6717−6724.
(15) Other dithiolate ligands referred to herein are 1,3-propanedithiolate (pdt) and 2-(mercaptomethyl)thiophenolate (mtp).
(16) Espenson, J. H.; Shan, X.; Wang, Y.; Huang, R.; Lahti, D. W.; Dixon, J.; Lente, G.; Ellern, A.; Guzei, I. A. *Inorg. Chem.* **2002**, *41*, 2583−2591.
(17) Takacs, J.; Cook, M. R.; Kiprof, P.; Kuchler, J. G.; Herrmann, W. A. *Organometallics* **1991**, *10*, 316−320.
(18) Blessing, R. H. *Acta Crystallogr.* **1995**, *51*, 33−38.
(19) All software and sources of the scattering factors are contained in the SHELXTL (version 5.1) program library (Sheldrick, G. M. S. *SHELXTL*, version 5.1; Bruker Analytical X-ray Systems: Madison, WI, 1997).

Table 1. Experimental Data for the X-ray Diffraction Studies of $PicH^+\mathbf{3}^-$ and **4**

	$PicH^+\mathbf{3}^-$	**4**
empirical formula	$C_{15}H_{20}NOReS_3$	$C_7H_{19}N_2OReS_3$
fw	512.72	441.64
a/Å	7.3826(5)	8.7615(12)
b/Å	9.7701(6)	16.426(3)
c/Å	12.8309(8)	10.0210(15)
α/deg	94.362(1)	
β/deg	102.414(1)	93.768(4)
γ/deg	99.639(1)	
V/Å^3	885.02(10)	1439.1(4)
Z	2	4
space group	$P\bar{1}$	$P2_1$
T/K	173(2)	293(2)
wavelength/Å	0.71073	0.71073
ρ_{calcd}/g cm^{-3}	1.924	2.038
μ/mm^{-1}	7.216	8.859
R indices (all data)[a]	R1 = 0.0237 wR2 = 0.0575	R1 = 0.0340 wR2 = 0.0711

[a] $R1 = \sum||F_o| - |F_c||/\sum|F_o|$; $wR2 = \{\sum[w(F_o^2 - F_c^2)^2]/\sum[w(F_o^2)^2]\}^{1/2}$.

were refined in full-matrix anisotropic approximation. All hydrogen atoms were placed in the structure factor calculation at idealized positions and were allowed to ride on the neighboring atoms with relative isotropic displacement coefficients.

Kinetics. LS reactions of **2**, $PicH^+\mathbf{3}^-$, $LutH^+\mathbf{3}^-$, and **4** with PPh_3 and pyridines were followed by monitoring the increase in absorbance in the range 380−420 nm from the buildup of the products MeReO(edt)PPh_3 and MeReO(edt)Py. The concentrations of the ligands were in at least 10-fold excess over rhenium. Thus, the absorbance−time data could be fitted to pseudo-first-order kinetics:

$$Abs_t = Abs_\infty + (Abs_0 - Abs_\infty) \times e^{-k_\psi \cdot t} \quad (3)$$

OAT reactions of **2**, **3**, and **4** with pyridine *N*-oxides were monitored by the change in absorbance at 400−500 nm, according to the identities of pyridine *N*-oxides and rhenium compounds. In most cases, the concentrations of the pyridine *N*-oxides were at least 100-times larger than those of rhenium compounds. Multiple-phase absorbance changes were observed. The reactions with **2** and **3** displayed a three-stage absorbance change: a fast rise and fall followed by a much slower further decrease, which was too sluggish to be studied. The kinetic data for the first two phases could be fitted to consecutive pseudo-first-order kinetics

$$Abs_t = Abs_\infty + \alpha \times e^{-k_\alpha \cdot t} + \beta \times e^{-k_\beta \cdot t} \quad (4)$$

where the two rate constants apply for the faster (k_α) and (k_β) slower steps.

In contrast, the reaction with compound **4** was a simplified version of reactions with **2** and **3**, with two stages: a fast rise that could be fitted to eq 3 and a slow decrease, not suitable for kinetic study, that spans about the same period of time as the third stage of reactions of **2** and **3**.

Results

Structural and Characterization Data. Table 1 presents the crystallographic parameters for $PicH^+\mathbf{3}^-$ and **4**, and Figure 1 depicts their molecular structures. In both compounds, the rhenium(V) atom lies in the center of a distorted square pyramid defined by the apical terminal oxo group and a basal plane occupied by a methyl group and three sulfur atoms from edt and SPh or tmtu. Important bond lengths and angles are summarized in Table 2. Irrespective of the negative charge on $PicH^+\mathbf{3}^-$, the Re≡O distances are identical at 169 pm for $PicH^+\mathbf{3}^-$ and **4**. The values of ν(Re−O) from the IR studies fall in the narrow range 976−1003 cm^{-1}, indicating that the ionic charge does not greatly influence the Re≡O bond. The Re−C distances are barely different, 215 pm in $PicH^+\mathbf{3}^-$ and 213 pm in **4**. Also, the ^{13}C chemical shifts of the CH_3 group are δ 7.2 for $PicH^+\mathbf{3}^-$, 6.8 for **4**; the CH_3 ^{1}H resonance is more sensitive to the ligand environment, lying at δ 2.38 for $PicH^+\mathbf{3}^-$ and 3.25 for **4**.

Table 2. Selected Bond Lengths (pm) and Angles (deg) of $PicH^+\mathbf{3}^-$ and **4**

	$PicH^+\mathbf{3}^-$	**4**
Re−O	169.2(3)	168.0(8)
Re−C(1)	215.4(4)	212.8(11)
Re−S(1)	233.49(10)	236.6(3)
Re−S(2)	232.49(9)	230.2(3)
Re−S(3)	229.65(9)	226.4(3)
O−Re−C(1)	107.14(16)	107.6(4)
O−Re−S(1)	109.48(10)	107.4(3)
O−Re−S(3)	108.59(10)	109.2(3)
C(1)−Re−S(2)	139.72(14)	137.3(3)
S(1)−Re−S(3)	140.85(4)	142.54(11)

In the solid state, $PicH^+\mathbf{3}^-$ is a salt. The 2 pm elongations of Re−S(2) and Re−S(3) may be attributable to the negative charge on $PicH^+\mathbf{3}^-$. On the basis of the orientation of the N−H group and the N···S(2) nonbonded distance, 319 pm, it appears that a hydrogen bond (N−H···S) exists between N and S(2). Such an interaction between a bridging thionate sulfur and a thioamide nitrogen was discovered in a copper complex with a N···S distance of 349 pm.[20] Two types of N−H···S hydrogen bonds were found in $(TACN)_2Fe_2S_6$: a "strong" interaction with d_{SH} = 231 pm and a "weak" interaction with d_{SH} = 265 pm.[21] In the present case, the calculated position of H gives an angle of 170.3° for N−H···S(2) and d_{SH} = 232 pm. From these comparisons, we conclude that a "strong" hydrogen bond interaction exists in $PicH^+\mathbf{3}^-$.

The infrared spectrum of $PicH^+\mathbf{3}^-$ was determined in chloroform. Neither an S−H nor an N−H frequency was found. This can be interpreted as indicating the presence of a pair of molecular species, Pic and **3**−H, in which a proton has been transferred to a coordinated thiolate ligand. Only when excess 2-picoline had been added was there recorded a strong, broad band at 3125 cm^{-1} characteristic of the Pic−H stretching vibration. In solutions containing excess 2-picoline, therefore, the $PicH^+\mathbf{3}^-$ ion pair is the predominant species. With other pyridines (Py) added to $PicH^+\mathbf{3}$, the predominant species will be $PyH^+\mathbf{3}$, by virtue of the concentration excess of Py and possibly its higher Brønsted basicity as well. The absence of an S−H vibration is probably due to its expected low intensity.

LS Reactions of 4. Substitution of tmtu by PPh_3 and 4-$Me_2NC_5H_4N$ yields [MeReO(edt)(PPh_3)] and [MeReO-

(20) Raper, E. S.; Creighton, J. R.; Clegg, W.; Cucurull-Sanchez, L.; Hill, M. N. S.; Akrivos, P. D. *Inorg. Chim. Acta* **1998**, *271*, 57−64.
(21) Francois, S.; Rohmer, M.-M.; Benard, M.; Moreland, A. C.; Rauchfuss, T. B. *J. Am. Chem. Soc.* **2000**, *122*, 12743−12750.

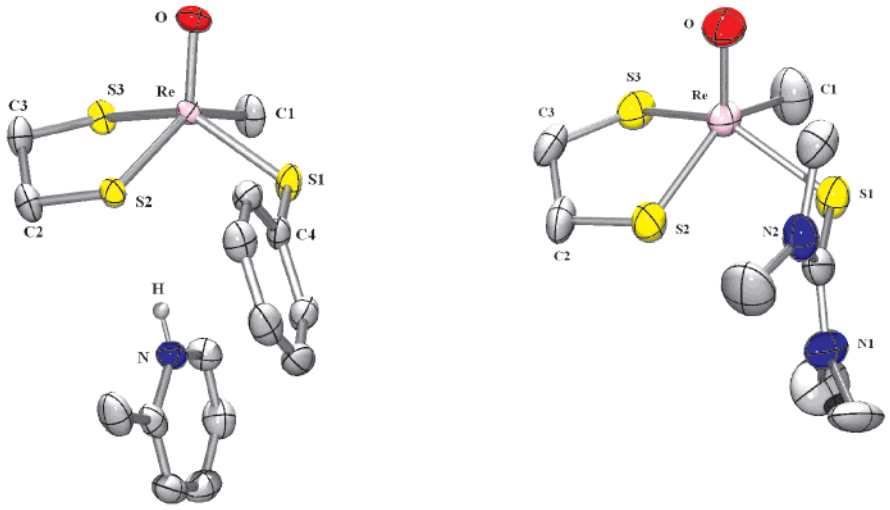

Figure 1. Crystallographically determined structures of $PicH^+3^-$ and **4**.

Scheme 1. Reactions of [MeReO(edt)(tmtu)], **4**, with Pyridine−Phosphine Mixtures

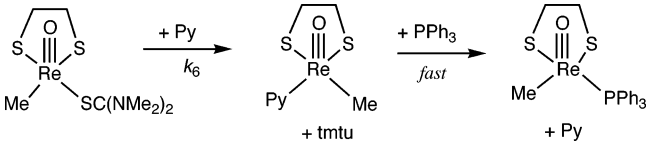

(edt)Py], eqs 5−6.

$$\mathbf{4} + PPh_3 \rightarrow [MeReO(edt)PPh_3] + tmtu \quad (5)$$

$$\mathbf{4} + Py \rightarrow [MeReO(edt)Py] + tmtu \quad (6)$$

The products are known from previous studies and were identified by their ^1H NMR spectra.[22] Both entering ligands are better Lewis bases than tmtu and were used in large stoichiometric excess, [L′] ≫ [**4**]; thus, the reactions proceeded to completion. The kinetics was straightforward:

$$-\frac{d[\mathbf{4}]}{dt} = \frac{d[MeReO(edt)L']}{dt} = k\cdot[\mathbf{4}]\cdot[L'] \quad (7)$$

Analysis of the data by first-order kinetics, eq 3, resulted in values of k_ψ that defined a straight line that passed through the origin. The slopes of these lines gave these rate constants, k/L mol^{-1} s^{-1}: $k_5 = 0.0820(6)$ and $k_6 = 20.1(2)$ for Py = 4-$Me_2NC_5H_5N$ at 25.0 °C in $CHCl_3$.

Further, pyridines accelerate the reaction between **4** and PPh_3. This phenomenon allows the evaluation of k_6 for 4-NCC_5H_4N and 2-MeC_5H_4N, which do not otherwise react with **4** to any great extent owing to electronic and steric factors, respectively. The initially formed [MeReO(edt)Py] then reacts with PPh_3 much more rapidly. Consequently, the k_6 step of Scheme 1 is rate-controlling, and the pseudo-first-order rate constants are directly proportional to [Py]. The slopes give k_6/L mol^{-1} s^{-1} = 0.095(1) for 4-NCC_5H_4N and 0.0103(3) for 2-MeC_5H_4N. Each step depicted in Scheme 1 leads to racemization accompanying LS, as demonstrated previously.[14]

When 4-$Me_2NC_5H_4N$ and PPh_3 were used concurrently, biexponential kinetics was followed, and the intermediate [MeReO(edt)(4-$Me_2NC_5H_4N$)] was observed to form and disappear. The rate constants were determined by fitting the data to eq 4. Values of the larger rate constant are linearly dependent on [4-$Me_2NC_5H_4N$], with $k_6 = 19.2(3)$. The second-stage reaction between [MeReO(edt)(4-$Me_2NC_5H_4N$)] and PPh_3 has $k = 33(1)$ L mol^{-1} s^{-1}. The values of these rate constants can be compared with the independent and presumably more reliable values, 20.1(2) L mol^{-1} s^{-1} and 28.0(5) L mol^{-1} s^{-1}, respectively.

LS Reactions of $PicH^+3^-$. These can be divided into two categories. First, there are the reactions with rate laws analogous to eq 7. Plots of k_ψ against [L′] are shown in Figure 2a. This pattern holds for L′ = PPh_3, 2,2′-bpy, and 1,10-phen, the respective rate constants for which are 2.57(2), 9.84(2), and 3.14(3) L mol^{-1} s^{-1} in chloroform at 25.0 °C.

We attribute the 30-fold slower reaction of **4** to the steric hindrance of tmtu. Both rate constants are relatively small compared with that for the reaction of MeReO(edt)(C_5H_4N) with PPh_3, with $k = 127$ L mol^{-1} s^{-1} in C_6H_6.[23] The mechanism of the PPh_3 reaction appears to be the same as that attributed earlier to eq 5. We do hesitate, however, in making the same statement about the reactions of bpy and phen, in light of the results now to be set forth.

In the second reaction category, we find all of the pyridines react according to

$$PicH^+3^- + XC_5H_4N \rightarrow [MeReO(edt)(NC_5H_4X)] + PhSH + 2\text{-Pic} \quad (8)$$

The rate shows a second-order dependence on [Py]

$$-\frac{d[PicH^+3^-]}{dt} = k_8\cdot[PicH^+3^-]\cdot[Py]^2 \quad (9)$$

as illustrated in Figure 2b. The third-order rate constants are $k_8 = 1.02(2) \times 10^6$ (4-$Me_2NC_5H_4N$) and $7.4(1) \times 10^3$ (4-PhC_5H_4N) L^2 mol^{-2} s^{-1}. The 2-order-of-magnitude dif-

(22) Lente, G.; Shan, X.; Guzei, I. A.; Espenson, J. H. *Inorg. Chem.* **2000**, *39*, 3572−3576.

(23) Shan, X.; Espenson, J. H. *Dalton Trans.* **2003**, 3612−3616.

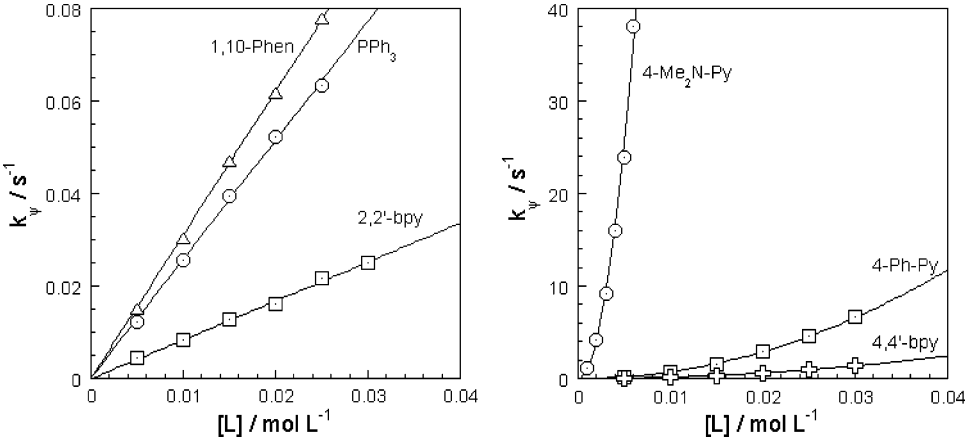

Figure 2. Plots of the pseudo-first-order rate constants in $CHCl_3$ at 25 °C for the reactions of $PicH^+\mathbf{3}^-$ against the concentrations of ligands: (a) PPh_3, 2,2′-bpy, and 1,10-Phen; and (b) 4-Me_2N-Py, 4-Ph-Py, and 4,4′-bpy.

ference between these values of k_8 indicates a substantial electronic effect from the substituents on pyridine, which is cumulative because two molecules of pyridine are involved in the third-order reactions. The reaction of $PicH^+\mathbf{3}^-$ with the nonchelating ligand 4,4′-bpy also follows third-order kinetics, Figure 2b, with $k_8 = 1.53(2) \times 10^3$ L^2 mol^{-2} s^{-1}.

Reaction 8 does not occur to an appreciable extent with 4-NCC_5H_5N or 2-MeC_5H_4N, no doubt for electronic and steric reasons, respectively. The reaction between {MeReO(edt)}$_2$ (**2**) and 4-PhC_5H_4N obeys the rate law $v = k[\mathbf{2}]\cdot[4\text{-}PhC_5H_4N]^2$, with $k = 2.76(3) \times 10^4$ L^2 mol^{-2} s^{-1}. The rate constant for **2** is four times larger than that for the reaction between 4-PhC_5H_4N and $PicH^+\mathbf{3}^-$.

The origin of the pyridine dependence in eq 9 will be discussed in a later section, but first it will be noted that monodentate pyridine ligands affect the LS reaction between $PicH^+\mathbf{3}^-$ and PPh_3. Although 4-NCC_5H_4N and 2-MeC_5H_4N (**B** in general) do not react with $PicH^+\mathbf{3}^-$, they do accelerate the reaction between $PicH^+\mathbf{3}^-$ and PPh_3. No MeReO(edt)Py was produced. The absence of a pyridine product comes as no surprise for two reasons. First, MeReO(dithiolate)PPh_3 is favored thermodynamically as shown in reaction 10. Second, MeReO(dithiolate)Py reacts rapidly with PPh_3, according to the values of k_{10}:

$$\text{MeReO(dithiolate)(4-}XC_5H_4N) + PPh_3 = \text{MeReO(dithiolate)}PPh_3 + XC_5H_4N \quad (10)$$

$$K\,(4\text{-}MeC_5H_4N) = 9.6 \times 10^2\,(\text{mtp});^{13}\ \text{ca. } 4 \times 10^1\,(\text{edt})^{23}$$

$$K\,(4\text{-}NCC_5H_4N) = 8 \times 10^3\,(\text{pdt})^{23}$$

$$k_{10}/\text{L mol}^{-1}\,\text{s}^{-1}\,(4\text{-}NCC_5H_4N) = 4.0 \times 10^2\,(\text{pdt});\ 4.8 \times 10^2\,(\text{edt})$$

When $[PPh_3]$ was kept constant at 10 mM, the pseudo-first-order rate constant rises with [**B**] and saturates at higher concentrations, Figure 3. The data, including the rate constants for reactions without **B** added, were fitted to eq 11 by using the computer program Scientist,[24] affording $K = 240(40)$, $k_2 = 3.1(1)$ L mol^{-1} s^{-1} for 4-NCC_5H_4N, and $K = 23(8)$, $k_2 = 1.7(9)$ L mol^{-1} s^{-1} for 2-MeC_5H_4N, and $k_1 = 2.58(5)$ L mol^{-1} s^{-1}, the same for both. The latter agrees with the directly determined value, $k_1 = 2.57(2)$ L mol^{-1} s^{-1}. With 4-NCC_5H_4N, the saturation behavior is indisputable, whereas with 2-Pic a smaller extent of curvature (and a correspondingly larger standard error in K) was noted. It is only to provide consistency with the former case that saturation is assumed to apply to both.

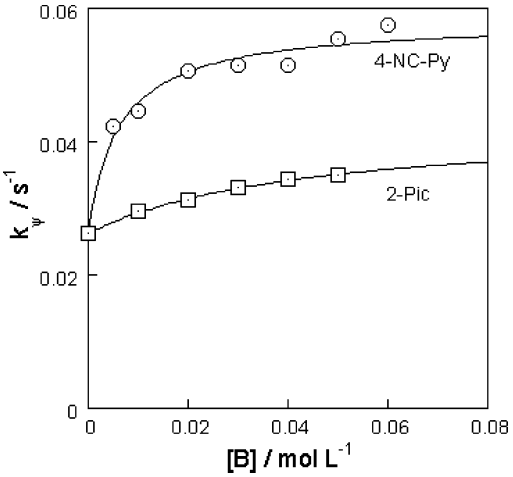

Figure 3. Plots of the pseudo-first-order rate constants for reactions of $PicH^+\mathbf{3}^-$ with PPh_3 in the presence of 4-NC-Py and 2-Me-Pic against [**B**] in $CHCl_3$ at 25 °C.

$$k_\psi = k_1[PPh_3] + \frac{k_2K[\mathbf{B}]}{1 + K[\mathbf{B}]}[PPh_3] \quad (11)$$

In the case of 4-PhC_5H_4N, one encounters not only its aforementioned reaction with $PicH^+\mathbf{3}^-$, $k_8 = 7.37(5) \times 10^3$ L^2 mol^{-2} s^{-1}, but also its additional effect on the reaction between $PicH^+\mathbf{3}^-$ and PPh_3. In this case, [MeReO(edt)(4-PhC_5H_4N)] formed and then vanished in two stages. With both ligands in stoichiometric excess over rhenium, the data were fitted to biexponential kinetics, eq 4. The larger pseudo-first-order rate constant k_α was directly proportional to [4-Ph-Py]^2 and k_β to $[PPh_3]$. The reaction steps and their rate constants are given in eq 12, which illustrates the agreement between the resolution of the stepwise model and the more reliable rate constants from

(24) *Scientist, 2.0*; Micromath Software, 1995.

the separate study of each step.

$$\text{PicH}^+\mathbf{3}^- \xrightarrow[2(4\text{-PhC}_5\text{H}_4\text{N})]{k_{12a}}$$

$$\text{PhSH} + \text{MeReO(edt)(NC}_5\text{H}_4\text{-Ph)} \xrightarrow[\text{PPh}_3]{k_{12a}}$$

$$\text{MeReO(edt)PPh}_3 + 4\text{-PhC}_5\text{H}_4\text{N}$$

Biexponential fitting:

$k_{12a} = 6.8(1) \times 10^3\ \text{L}^2\ \text{mol}^{-2}\ \text{s}^{-1}$ $k_{12b} = 98(1)\ \text{L mol}^{-1}\ \text{s}^{-1}$

Each independently:

$k_{12a} = 7.4(1) \times 10^3\ \text{L}^2\ \text{mol}^{-2}\ \text{s}^{-1}$ $k_{12b} = 96(1)\ \text{L mol}^{-1}\ \text{s}^{-1}$ (12)

Pyridine-Assisted LS Reactions of Py. Both 4-NCC_5H_4N and 2-MeC_5H_4N accelerate the reaction of $PicH^+\mathbf{3}^-$ with 4-Me_2N-Py, but without rate saturation even at high [**B**]. The rate is given by

$$v = k_{13}\cdot[\text{PicH}^+\ \mathbf{3}]\cdot[\text{Me}_2\text{NPy}]\cdot[\mathbf{B}] \quad (13)$$

with $k_{13} = 5.8(1) \times 10^4$ (**B** = 4-NCC_5H_4N) and 88(18) $L^2\ mol^{-2}\ s^{-1}$ (2-MeC_5H_4N). As before, there is a third-order rate law.

Influence of the Cation. This factor was investigated by using $LutH^+\mathbf{3}^-$ in reactions with Ph_3P and 4-Ph-Py. The results are identical with those for $PicH^+\mathbf{3}^-$, with $k_5 = 2.53(3)$ L $mol^{-1}\ s^{-1}$ and $k_8 = 7.14(9) \times 10^3\ L^2\ mol^{-2}\ s^{-1}$ for $LutH^+\mathbf{3}^-$, as compared with 2.57(2) and $7.37(5) \times 10^3$ for $PicH^+\mathbf{3}^-$. Addition of pyridinium ions had no effect on the kinetics. The reactions and rate constants are summarized in Table 3.

LS and OAT Reactions with Pyridine N-Oxides. When $PicH^+\mathbf{3}^-$ reacts with pyridine *N*-oxides, a three-stage absorbance change was observed, according to this sequence. First, a pyridine *N*-oxide replaces the SPh^- ligand:

$$\text{PicH}^+\mathbf{3}^- + \text{PyO} \rightarrow \text{MeReO(edt)(OPy)} + \text{PhSH} + \text{2-Pic} \quad (14)$$

$$\text{MeReO(edt)(OPy)} + \text{PyO} \rightarrow [\text{MeReO(edt)(OPy)}_2] \rightarrow \text{MeRe(O)}_2\text{(edt)(OPy)} + \text{Py} \quad (15)$$

Following that, slow decomposition of the dioxorhenium(VII) intermediate sets in:

$$\text{MeRe(O)}_2\text{(edt)(OPy)} \rightarrow \text{MeReO}_3 + \text{Py} + \text{RSSR} \quad (16)$$

The UV−vis spectra of the species involved are given in Figure 4. This scheme was deduced not only from the kinetic pattern, but also by induction from the reactions of related species.[5−7,16]

Reaction 16 was too sluggish for kinetic study. The first two stages of absorbance change were fitted to eq 4, giving two pseudo-first-order rate constants, designated k_α and k_β ($k_\alpha > k_\beta$). Figure 5 depicts the plots of the pseudo-first-order rate constants for oxidation of $PicH^+\mathbf{3}^-$ against concentrations of pyridine *N*-oxides.

Both rate constants vary linearly with [PyO]. Rate constants of oxidation of $PicH^+\mathbf{3}^-$ by pyridine *N*-oxides are summarized in Table 4. The rate constants span these ranges: $k_{14}/10^4$ L $mol^{-1}\ s^{-1} = 0.23-12$ and $k_{15}/10^3$ L $mol^{-1}\ s^{-1} = 0.3-8$. The Hammett analysis for $PicH^+\mathbf{3}^-$ shows large reaction constants, $\rho_{14} = -5.3 \pm 1.1$ and $\rho_{15} = -4.3 \pm 0.8$, as illustrated in Figure 6.

Table 3. Summary of Kinetic Data for $PicH^+\mathbf{3}^-$ and **4**

L	*n* value (for $[L]^n$)	$PicH^+\mathbf{3}^-$ $k/L^{n-1}\ mol^{1-n}\ s^{-1}$	**4** $k/L\ mol^{-1}\ s^{-1}$
4,4′-bpy	2	$1.53(2) \times 10^3$	
1,10-phen	1	3.14(3)	
PPh_3	1	2.57(2)	$8.20(6) \times 10^{-2}$
2,2′-bpy	1	0.84(2)	
4-$Me_2NC_5H_4N$	2	$1.02(6) \times 10^6$	
4-$Me_2NC_5H_4N$	1		20.1(2)
4-PhC_5H_4N	2	$7.37(5) \times 10^3$	
4-NCC_5H_4N	1		$9.5(1) \times 10^{-2}$
2-MeC_5H_4N	1		$1.03(3) \times 10^{-2}$
4-$Me_2NC_5H_4N$ + 4-NCC_5H_4N	1 + 1	$5.8(1) \times 10^4$	
4-$Me_2NC_5H_4N$ + 2-MeC_5H_4N	1 + 1	88(2)	
PPh_3 + 4-NCC_5H_4N	eq 11	$K = 2.4(4) \times 10^2$, $k_2 = 3.1(1)$	
PPh_3 + 2-MeC_5H_4N	eq 11	$K = 23.8(1)$, $k_2 = 1.7(9)$	

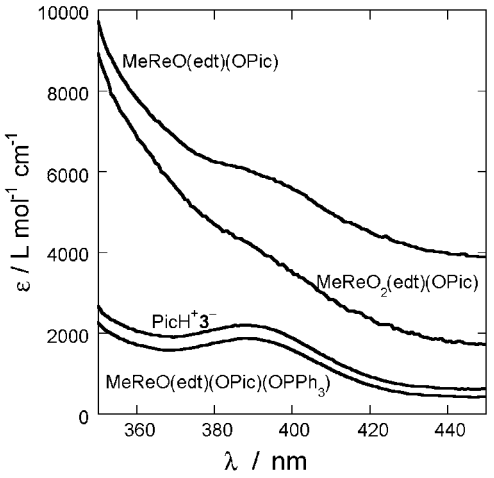

Figure 4. Spectra of $PicH^+\mathbf{3}^-$ and the intermediates MeReO(edt)(OPic) and $MeRe(O)_2$(edt)(OPic), and the product from the reaction of the latter with PPh_3, MeReO(edt)(OPic)($OPPh_3$). (Note: 2-Pic is present in the starting complex, and the reagent is 4-PicO, which is the ligand in these species.)

This analysis leaves unanswered the question of which of k_α or k_β corresponds to eq 14 or 15, although the designations in the final sentence of the preceding paragraph give our conclusions formed from the analysis to follow. To identify which rate constant is which, **2** was used to react with 4-$MeOC_5H_4NO$ and 4-PhC_5H_4NO. Three-stage absorbance changes were observed, like those in eqs 14−16 for $PicH^+\mathbf{3}^-$. The first two stages were fitted to eq 4, affording k_α and k_β. Varying the concentrations of two PyO species, k_α shows mixed first-order and second-order dependences on [PyO], $k_\alpha = k_{1a}[\text{PyO}] + k_{1b}[\text{PyO}]^2$, affording $k_{1a} = 1.27(8) \times 10^4$ L $mol^{-1}\ s^{-1}$ and $k_{1a} = 8(6) \times 10^4\ L^2\ mol^{-2}\ s^{-1}$ for 4-$MeOC_5H_4$-NO and $k_{1a} = 6.5(3) \times 10^3$ L $mol^{-1}\ s^{-1}$ and $k_{1a} = 1.4(2) \times 10^5\ L^2\ mol^{-2}\ s^{-1}$ for 4-PhC_5H_4NO. Unlike k_α, k_β varies linearly with [PyO], giving second-order rate constants, 1.70(3) $\times 10^4$ L $mol^{-1}\ s^{-1}$ for 4-$MeOC_5H_4NO$ and $1.32(1) \times 10^3$ for 4-PhC_5H_4NO. The monomerization of **2** follows mixed first-order and second-order kinetics.[13,16] Unmistakably, therefore, k_α applies to eq 14.

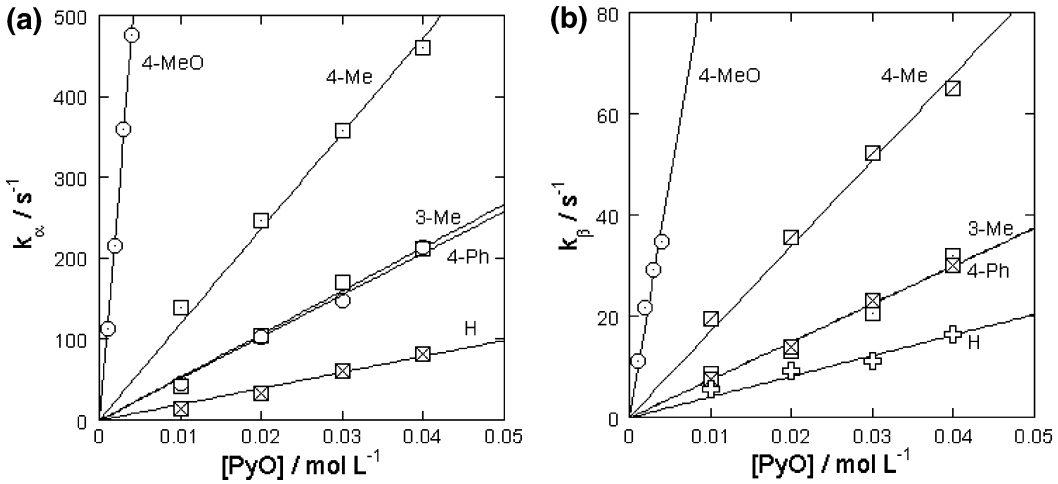

Figure 5. Plots of (a) k_α and (b) k_β against [PyO] for the reaction between $PicH^+\mathbf{3}^-$ and pyridine *N*-oxides in $CHCl_3$ at 25 °C.

Table 4. Rate Constants for the Oxidation of $PicH^+\mathbf{3}^-$ and **4** by Pyridine *N*-Oxides[a]

X (as in X-C_5H_4NO)	$PicH^+\mathbf{3}^-$ $k_{14}/10^3$ [b]	$k_{15}/10^3$ [b]	**4** k_1 [b]	**2** $k_{1a}/10^3$ [b]	**2** $k_{1b}/10^4$ [c]	**2** $k_2/10^3$ [b]
4-MeO	123(6)	7.9(8)	20.5(5)	12.7	8(6)	17.0
4-Me	10.7(1)	1.53(6)	3.58(3)			
3-Me	5.8(4)	0.78(11)	1.27(2)			
4-Ph	5.5(3)	0.77(4)	1.34(2)	6.5	14	1.32
H	2.3(1)	0.34(4)	0.84(1)			
ρ	-5.3 ± 1.1	-4.3 ± 0.8	-4.7 ± 0.7			

[a] At 25.0 °C in chloroform. [b] L mol^{-1} s^{-1}. [c] L^2 mol^{-2} s^{-1}.

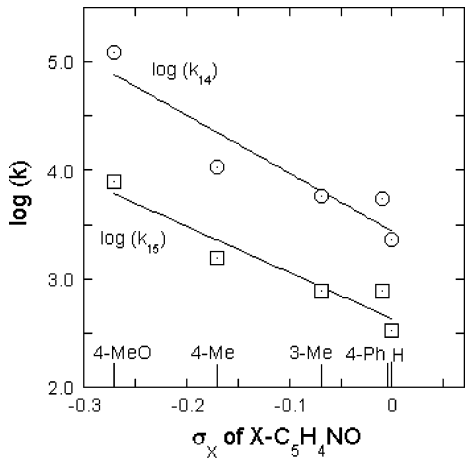

Figure 6. Hammett analysis of the effects of pyridine *N*-oxide substituents on the rate constants (Table 4) for LS (k_{14}) and OAT (k_{15}) of $PicH^+\mathbf{3}^-$ at 25.0 °C in chloroform.

LS and OAT reactions of **4** with PyO are much slower than those of $PicH^+\mathbf{3}^-$. The absorbance change occurs in two stages, the second of which corresponds to the third stage of the $PicH^+\mathbf{3}^-$ reaction, namely the decomposition of $MeRe(O)_2(edt)(OPy)$, eq 16. The first stage shows a first-order dependence on [PyO], affording second-order rate constants in the range 0.8−21 L mol^{-1} s^{-1} (Table 4). A Hammett analysis gave $\rho = -4.7 \pm 0.7$, also indicative of an unusually large substituent effect.

Although the decomposition of $MeRe(O)_2(edt)OPy$ is too sluggish for kinetics, the relative rate can be estimated by the time for complete reaction. The rate did not depend on [PyO] but did depend on the identity of the pyridine *N*-oxide. The rate for 4-PhC_5H_4NO is about two times slower than that for 4-PicO. When PPh_3 was added to the solution of $MeRe(O)_2(edt)OPy$, the absorbance changed nearly instantaneously, as the catalytic cycle transfers an oxygen atom from PyO to PPh_3 according to the stoichiometric reaction of eq 1 and step 17.

$$MeRe(O)_2(edt)(OPy) + PPh_3 \rightarrow MeRe(O)(edt)(OPPh_3) + PyO \quad (17)$$

Figure 4 depicts the spectrum of MeReO(edt)(4-OPic)-$(OPPh_3)$, the product of this reaction. The weak ligand Ph_3-PO can readily be replaced by PyO. Although this metastable species was not structurally characterized, certain Re−$OPPh_3$ comparison compounds have been found in the literature.[8,25,26] $Re(O)Cl_3(OPPh_3)(Me_2S)$ was used as a catalyst for oxygenation of thiols.[8] $[(HCpz_3)ReCl_2(OPPh_3)]Cl$ and $(HBpz_3)$-$ReCl_2(OPPh_3)$ were formed from the oxygen abstraction of PPh_3 from corresponding rhenium(V) complexes, $(HCpz_3)$-$ReOCl_2$ and $(HBpz_3)ReOCl_2$.[26] Analogous Mo and W compounds were also found and structurally characterized, such as $[LMo^{IV}(OPR_3)(p\text{-}OC_6H_4{-}OC_2H_5)_2]^+$ and *anti*-$Cl_2O(Ph_3PO)W(\mu\text{-S-}i\text{-Bu})_2W(Ph_3PO)Cl_2O$.[25] The reaction of $MeRe(O)_2(edt)OPy$ with PPh_3 is too fast for stopped-flow kinetics, giving a conservative limit on the second-order rate constant $k_{17} > 6 \times 10^5$ L mol^{-1} s^{-1}.

Discussion

The N-H···S Hydrogen Bond. This interaction has been recognized in metalloproteins, electron-transfer iron−sulfur proteins,[27] and cytochrome P450 compounds with thiolate−metal coordination,[28] where it maintains structures and modulates redox potentials of metal centers. Models containing Fe, Co, Mo were synthesized, and a variety of N−H···S hydrogen bonds were discovered and characterized.[29,30] Most of them contain a bent hydrogen bond with an N−H···S angle <180°.[29] In only a few cases has an angle close to 180° been observed.[30] To our knowledge, the N−H···S

(25) (a) Ball, J. M.; Boorman, P. M.; Richardson, J. F. *Inorg. Chem.* **1986**, *25*, 3325−3327. (b) Nemykin, V. N.; Davie, S. R.; Mondal, S.; Rubie, N.; Kirk, M. L.; Somogyi, A.; Basu, P. *J. Am. Chem. Soc.* **2002**, *124*, 756−757.

(26) Seymore, S. B.; Brown, S. N. *Inorg. Chem.* **2000**, *39*, 325−332.

hydrogen bond in $PicH^+\mathbf{3}^-$ is the first case of this interaction in a rhenium complex.

Mechanistic Interpretation of LS Reactions. The studies of **4** gave results that parallel those for other reactions between [MeReO(dithiolate)L] and L′ for various ligand combinations, including L = Py, L′ = PAr_3; L = Py, L′ = Py′; L = PAr_3 and L′ = PAr_3′, and others.[11,14] The collective assessment of these data allows the assignment of associative mechanisms to the LS reactions, in these and in the previous instances. The bases for this are, among other factors, that the rate constants reported previously[11,13] are strongly dependent on the identities of the entering ligands and characterized by large, negative values of $\Delta S^{\ddagger}$.

The important issue is to find a plausible and hopefully correct explanation for the second-order dependences on [Py] in eqs 9 and 13. Only $PicH^+\mathbf{3}^-$ gives rise to this rate law; all other reactions of [MeReO(dithiolate)L] + L′ (here and in previous studies[11,13,23]) follow second-order kinetics. To show that we have made a thoughtful analysis of the problem, we will present a number of possibilities, some of which are not entirely credible. In doing so, it must be kept in mind that the mechanism must also accommodate data for the chelating ligands 2,2′-bpy and 1,10-phen. That being said, two pyridine nitrogen atoms must each have a role to play, whether from a chelating ligand or from two monodentates. Here are the possibilities uncovered by the analysis, and a discussion of each.

(a) The reaction entails a seven-coordinated rhenium atom in the transition state, $[PicH^+MeRe(O)(edt)(SPh)(Py)_2]^{\ddagger}$, the steps and rate law being as follows:

$$PyH^+\mathbf{3}^- + Py = PyH^+\mathbf{3}^-\cdot Py \ (K_1)$$

$$PyH^+\mathbf{3}^-\cdot Py + Py \rightarrow PyH^+\mathbf{3}^-\cdot Py_2 \ (k_2)$$

$$PyH^+\mathbf{3}^-\cdot Py_2 \rightarrow MeReO(edt)Py + PhSH + Py \ (fast)$$

$$k_{obs} = \frac{k_1 k_2 [Py]^2}{k_1[Py] + k_{-1} + k_2[Py]}$$

Because the formation of the seven-coordinated species $PyH^+\mathbf{3}^-\cdot Py_2$ is the most sterically hindered step, k_2 must be small. Thus, $k_1[Py] + k_{-1} \gg k_2[Py]$. Further, $k_{-1} \gg k_1$, so in the limit

$$k_{obs} = \frac{k_1 k_2 [Py]^2}{k_{-1}}$$

The data cannot directly negate this mechanism, but strong arguments can be advanced against it. For one thing, no other LS reaction has a transition state with a seven-coordinate structure. Moreover, the anionic charge on $\mathbf{3}^-$ should, in particular, disinvite the coordination of two Lewis bases.

(b) The reaction involves the conversion of $PicH^+\mathbf{3}^-$ to $PyH^+\mathbf{3}^-$ in a prior equilibrium, $PicH^+\mathbf{3}^- + Py = PyH^+\mathbf{3}^- + Pic$, the species so formed then reacting with the second Py. Unless the prior equilibrium lay well toward $PicH^+\mathbf{3}^-$, which can hardly be the case, given the relative concentrations and Lewis basicities of Pic and Py, this mechanism will not fit the kinetic data. The difficulty is that the new rhenium reagent, $PyH^+\mathbf{3}^-$, will be the predominant reactant and as such will not give rise to a dependence on [Py]. This proposal still cannot reconcile eqs 9 and 13. Nonetheless, it points to another issue, that the real rhenium reactant in the pyridine reactions is $PyH^+\mathbf{3}^-$.

Scheme 2. Proposed Mechanism for Reactions between $PyH^+\mathbf{3}^-$ and Pyridines

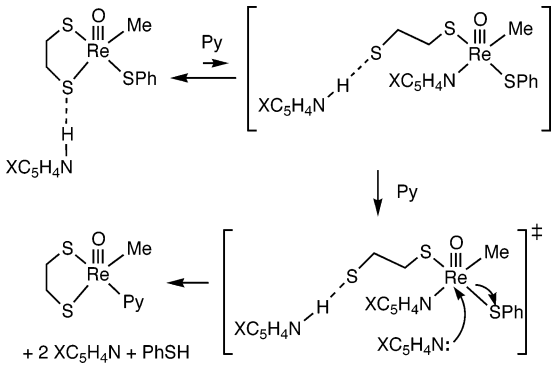

(c) The reaction is preceded by dissociation of $PyH^+\mathbf{3}^-$ to the molecular species Py and **3**, as could be favored in chloroform, with the proton residing on the sulfur atom of the alkanethiolate ligand. Attack of one Py at the S−H proton and the other at the rhenium might then advance the reagents toward the transition state. Once solution IR spectroscopy showed ν_{NH} in the absence of added pyridine, this proposal became untenable.

(d) Equilibrium coordination of one Py to rhenium results in release of that arm of the dithiolate chelate to which $PyH^+\mathbf{3}^-$ was hydrogen-bonded. The position of equilibrium must lie to the left for consistency with the kinetic data. This is a plausible transformation, in that a thiol RSH is formed from a thiolate; dechelation is further favored by the trans influence of the methyl ligand (refer to Figure 1). The second Py could attack at the still-vacant sixth coordination position. Accompanying loss of PhSH, the products would be formed rapidly. This mechanistic sequence is illustrated in Scheme 2. It is to be understood that the donor atoms of the ligands 2,2′-bpy and 1,10-phen play both roles, and thus show a reaction order of unity.

(27) (a) Nakamura, A.; Ueyama, N. *Adv. Inorg. Chem.* **1989**, *33*, 39−67. (b) Denke, E.; Merbitz-Zahradnik, T.; Hatzfeld, O. M.; Snyder, C. H.; Link, T. A.; Trumpower, B. L. *J. Biol. Chem.* **1998**, *273*, 9085−9093. (c) Bertini, I.; Felli, I.; Kastrau, D. H. W.; Luchinat, C.; Piccioli, M.; Viezzoli, M. S. *Eur. J. Biochem.* **1994**, *225*, 703−714. (d) Blake, P. R.; Park, J. B.; Adams, M. W. W.; Summers, M. F. *J. Am. Chem. Soc.* **1992**, *114*, 4931−4933. (e) Sheridan, R. P.; Allen, L. C.; Carter, C. W., Jr. *J. Biol. Chem.* **1981**, *256*, 5052−5057.

(28) (a) Crane, B. R.; Arvai, A. S.; Gachhui, R.; Wu, C.; Ghosh, D. K.; Getzoff, E. D.; Stuehr, D. J.; Tainer, J. A. *Science* **1997**, *278*, 425−431. (b) Sundaramoorthy, M.; Terner, J.; Poulos, T. L. *Structure* **1995**, *3*, 1367−1377. (c) Cupp-Vickery, J. R.; Poulos, T. L. *Nat. Struct. Biol.* **1995**, *2*, 144−153.

(29) (a) Huang, J.; Ostrander, R. L.; Rheingold, A. L.; Leung, Y.; Walters, M. A. *J. Am. Chem. Soc.* **1994**, *116*, 6769−6776. (b) Walters, M. A.; Dewan, J. C.; Min, C.; Pinto, S. *Inorg. Chem.* **1991**, *30*, 2656−2662. (c) Okamura, T.-A.; Takamizawa, S.; Ueyama, N.; Nakamura, A. *Inorg. Chem.* **1998**, *37*, 18−28. (d) Ueyama, N.; Nishikawa, N.; Yamada, Y.; Okamura, T.-a.; Nakamura, A. *J. Am. Chem. Soc.* **1996**, *118*, 12826−12827.

(30) Suzuki, N.; Higuchi, T.; Urano, Y.; Kikuchi, K.; Uekusa, H.; Ohashi, Y.; Uchida, T.; Kitagawa, T.; Nagano, T. *J. Am. Chem. Soc.* **1999**, *121*, 11571−11572.

Certain presumptions have been built into the scheme as it is depicted, because no allowance for other isomers has been made; that is, there are no data pertaining to which isomeric forms of certain species are present. The pyridinium ion hydrogen bonded to a thiolate sulfur is depicted in the position established crystallographically, namely the sulfur trans to the methyl group, although there is no evidence that the solution and solid-state structures are the same. The subsequent equilibrium is presumed to give the isomer shown because it has been demonstrated earlier that isomerization about rhenium occurs during ligand substitution.[11] The sequence implicit here follows: addition of Py trans to the oxo group; turnstile rotation of the relevant donor atoms, namely Py, S of edt (that with PyH^+), and either the other S of edt or SPh. Either rotation will position the leaving S of edt trans to the oxo group. Because the choice between the other S of edt or SPh is arbitrary in the absence of data bearing on that point, we have assumed SPh is part to the rotating trio, which will lead to an intermediate having the structure shown. Product formation from the transition state constitutes another turnstile rotation, but the product is an enantiomer not a geometrical isomer. To spell out structural alternatives would confuse the point being made in Scheme 2; to present only line formulas in order to avoid explicit structures would make the presentation difficult to follow. Consequently, we have shown what seem to be reasonable structural isomers, while admitting that this is not an exclusive representation of the species.

The different kinetic patterns for phosphines (eq 11) and pyridines (eq 9) deserve further comment. When solutions lack excess pyridine, the rhenium species is $\mathbf{3}^-$, $[MeReO(edt)(SPh)]^-$. It will react with PPh_3 without edt ring-opening, by the associative mechanism described for many such compounds, that features the turnstile rotation step.[11] The data for pyridine substitutions, on the other hand, show that pyridine assists in the substitution by involvement of edt, Scheme 2.

OAT Reactions. The nucleophilic assistance on the severing of the O−Py bond was first discovered in the reduction of pyridine *N*-oxides with the catalyst $MeReO(mtp)PPh_3$.[5,6] With $PicH^+\mathbf{3}^-$, the three reaction stages are given by eqs 14−16. The first stage is a common ligand displacement in which pyridine *N*-oxide acts as a Lewis base,[31] showing a first-order dependence on [PyO]. The use of substituted pyridine *N*-oxides gave a large Hammett reaction constant, $\rho = -5.3$. The scission of the O−N bond of PyO coordinated to rhenium occurs in the second step with the nucleophilic assistance of a second PyO, giving rise to the reactive intermediate $[MeRe(O)_2(edt)(OPy)]$. The substituents on the first and second PyO provide the two large negative contributions to the reaction constant. The third step, nucleophilically assisted cleavage of the Py−O bond, would contribute a positive reaction constant, with Py as the leaving group, but it evidently contributes only in a minor way, because bond cleavage is not far advanced in the transition state.

An analogous dioxorhenium(VII) compound, $\{MeRe(O)_2\}_2\{-SCH_2CH(O)CH(O)CH_2S-\}$, has a distorted trigonal-bipyramidal structure with identical oxo groups.[16] The reaction of $MeRe(O)_2(OCH_2CH_2S)$ with PPh_3 occurs relatively slowly.[2] Similar to these, five-coordinate Mo(VI) complexes with two terminal oxo groups were recognized as key models for sulfite oxidase.[32] With 8-hydroxyqulinolinate, a six-coordinate dirhenium complex was synthesized from the condensation of methyltrioxorhenium(VII) with free ligands.[33] Similarly, the condensation of methyltrioxorhenium(VII) with diols and diamines affords dioxorhenium(VII) complexes with an extra Lewis base as the sixth ligand,[17,34] having cis oxo groups. In the catalytic OAT reaction, six-coordinate dioxorhenium species were proposed as the immediate oxidation products.[4] The dependence on the identity of PyO of the decomposition of this species indicates that PyO is coordinated. Thus, $MeRe(O)_2(edt)OPy$ is the product from the scission of the O−N bond.

As to why nucleophilic assistance is necessary, we note that the scission of the O−Py bond requires electron transfer from O to N. The inductive effect of another PyO promotes this step and also stabilizes the oxidation product. Electron-rich ligands are known to stabilize and lower the reactivity of the Re−O bond.[35]

The first step of the oxidations of **4** by PyO is much slower than the second, which is the same as the second step of oxidation of $PicH^+\mathbf{3}^-$. So, the reactions of **4** simplify into two stages, ligand displacement and decomposition of $MeRe(O)_2(edt)OPy$.

Acknowledgment. This research was supported by the U.S. Department of Energy, Office of Basic Energy Sciences, Division of Chemical Sciences, under Contract W-7405-Eng-82 with Iowa State University of Science and Technology. We are grateful to the reviewers for helpful comments on the mechanisms of the ligand substitution reactions.

Supporting Information Available: Crystallographic data and plots of kinetic data to illustrate agreement with selected mathematical forms and to evaluate numerical parameters. This material is available free of charge via the Internet at http://pubs.acs.org.

IC049772C

(31) (a) Batigalhia, F.; Zaldini-Hernandes, M.; Ferreira, A. G.; Malvestiti, I.; Cass, Q. B. *Tetrahedron* **2001**, *57*, 9669−9676. (b) Herrmann, W. A.; Correia, J. D. G.; Rauch, M. U.; Artus, G. R. J.; Kuehn, F. E. *J. Mol. Catal. A: Chem.* **1997**, *118*, 33−45. (c) Lichtenhan, J. D.; Ziller, J. W.; Doherty, N. M. *Inorg. Chem.* **1992**, *31*, 4210−4212. (d) Sensato, F. R.; Cass, Q. B.; Longo, E.; Zukerman-Schpector, J.; Custodio, R.; Andres, J.; Hernandes, M. Z.; Longo, R. L. *Inorg. Chem.* **2001**, *40*, 6022−6025.

(32) (a) Kisker, C.; Schindelin, H.; Pacheco, A.; Wehbi, W. A.; Garrett, R. M.; Rajagopalan, K. V.; Enemark, J. H.; Rees, D. C. *Cell* **1997**, *91*, 973−983. (b) Garrett, R. M.; Rajagopalan, K. V. *J. Biol. Chem.* **1996**, *271*, 7387−7391. (c) George, G. N.; Kipke, C. A.; Prince, R. C.; Sunde, R. A.; Enemark, J. H.; Cramer, S. P. *Biochemistry* **1989**, *28*, 5075−5080. (d) George, G. N.; Garrett, R. M.; Prince, R. C.; Rajagopalan, K. V. *J. Am. Chem. Soc.* **1996**, *118*, 8588−8592. (e) Peariso, K.; McNaughton, R. L.; Kirk, M. L. *J. Am. Chem. Soc.* **2002**, *124*, 9006−9007.

(33) Takacs, J.; Kiprof, P.; Kuchler, J. G.; Herrmann, W. A. *J. Organomet. Chem.* **1989**, *369*, C1−C5.

(34) (a) Takacs, J.; Kiprof, P.; Riede, J.; Herrmann, W. A. *Organometallics* **1990**, *9*, 782−787. (b) Wang, W.-D.; Ellern, A.; Guzei, I. A.; Espenson, J. H. *Organometallics* **2002**, *21*, 5576−5582.

(35) Gangopadhyay, J.; Sengupta, S.; Bhattacharyya, S.; Chakraborty, I.; Chakravorty, A. *Inorg. Chem.* **2002**, *41*, 2616−2622.